Available online at www.sciencedirect.com
SCIENCE DIRECT®
Carbohydrate Research 340 (2005) 459–468
Carbohydrate RESEARCH

DFT study of α- and β-D-mannopyranose at the B3LYP/6-311++G** level

Michael Appell, J. L. Willett and Frank A. Momany*

Plant Polymer Research, USDA,† ARS, National Center for Agricultural, Utilization Research, 1815 N. University Street, Peoria, IL 61604, USA

Received 20 September 2004; accepted 4 December 2004
Available online 13 January 2005

Abstract—Thirty-five conformations of α- and β-D-mannopyranose, the C-2 substituted epimer of glucopyranose, were geometry optimized using the density functional (B3LYP), and basis set (6-311++G**). Full geometry optimization was performed on the hydroxymethyl rotamers (*gg*/*gt*/*tg*) and an analytical hessian program was used to calculate the harmonic vibrational frequencies, zero point energy, enthalpy, and entropy. The lowest energy conformation investigated is the β-*tg* in the $^4C_1$ chair conformation. The in vacuo calculations showed little energetic preference for either the α or β anomer for mannopyranose in the $^4C_1$ chair conformation. Results are compared to similar glucopyranose calculations in vacuo where the α anomer is ~1 kcal/mol lower in electronic energy than the β anomer. In the case of the generally higher energy $^1C_4$ chair conformations, one low-energy, low-entropy β-*gg*-$^1C_4$ chair conformation was identified that is within ~1.4 kcal/mol of the lowest energy $^4C_1$ conformation of mannopyranose. Other $^1C_4$ chair conformations in our investigation are ~2.9–7.9 kcal/mol higher in overall energy. Many of the $^{3,O}B$, $B_{3,O}$, $^{1,4}B$, and $B_{1,4}$ boat forms passed through transitions without barriers to $^1S_3$, $^5S_1$, $^1S_5$ skew forms with energies between ~3.6 and 8.9 kcal/mol higher in energy than the lowest energy conformation of mannopyranose. Boat forms were found that remained stable upon gradient optimization. As with glucopyranose, the orientation and interaction of the hydroxy groups make a significant contribution to the conformation/energy relationship in vacuo.
Published by Elsevier Ltd.

Keywords: B3LYP/6-311++G**; Mannose; Glucose; Chair; Hessian; Relative free energy

1. Introduction

1.1. Background

In this work high-level density functional methods were used to study the conformational preferences of the $^4C_1$ and $^1C_4$ chair conformations as well as boat and skew–boat conformations of α- and β-D-mannopyranose. The purpose of this study is to investigate the effects of epimerization at the C-2 position on the energy/property relationships of carbohydrates, and apply these relationships in the design of new polymers with desired properties. Mannose is also of general interest as a component in biological systems.

To our knowledge, a study of mannopyranose of this scope and at this level has not been reported. Many computational studies on carbohydrates, including glucose and its epimers, or related substructures have appeared in the literature and will not be reviewed in detail in this paper.[1–24] However, work related to our calculations of mannopyranose will be compared with the results presented here.

The interactions and thus the geometries and relative energies among conformers of carbohydrates are known to be very dependent on selection of both the basis set and density functional with DFT calculations.[1–7] Energies obtained from a larger basis set using structures optimized with a smaller basis set do not necessarily correspond with energies and resulting geometries

* Corresponding author. Tel./fax: +1 309 681 6362; e-mail: momanyfa@ncaur.usda.gov

† Names are necessary to report factually on available data; however, the USDA neither guarantees nor warrants the standard of the product, and the use of the name by USDA implies no approval of the product to the exclusion of others that may also be suitable.

0008-6215/$ - see front matter Published by Elsevier Ltd.
doi:10.1016/j.carres.2004.12.010

optimized with a larger basis set. This inherent discrepancy was shown to lead to significant errors in optimized geometries and energies.[1] Also, differences in relative energies obtained from different basis sets on the same geometry of structures of glucose and its epimers have been reported,[2] and the inclusions of diffuse functions have been found to be important.[3] This dependence has also been reported for structures related to carbohydrates.[8]

DFT studies in this laboratory on glucose[4] in vacuo and monohydrates of glucose,[5] as well as maltose[1] and cellobiose in vacuo[6,7] have shown that the B3LYP/6-311++G** level of theory will give consistently reliable geometries and conformationally dependent energies for carbohydrates. To ensure that this is the case in the work presented here, all structures were geometry optimized at this level of theory (B3LYP/6-311++G**).

The conformational preferences of mannopyranose and its derivatives have been explored experimentally by ^{1}H NMR studies[18,24–26] and X-ray crystal structures.[27–30] The X-ray structure for α-D-mannopyranose showed that the molecule exists in the crystal environment in the $^4C_1$ chair conformation.[29] Hydrogen bonding has been shown to be prevalent in carbohydrate crystal structures with the hydroxy groups acting as both hydrogen bond donors and acceptors.[27–30] It has also been experimentally observed that the hydrogen bond network can form long, cooperative chains, linking the sugar molecules to water molecules when crystal hydrates are studied.[28]

The preference of mannopyranose for the $^4C_1$ chair conformation has also been observed in solution by NMR spectroscopy.[26] The anomeric ratio in solution was found to be 68:32 (α/β) by NMR spectroscopy.[26] This is opposite to the anomeric ratio of glucose in solution, where the β anomer is preferred. An investigation into the rotamer population of pseudo-D-mannose by ^{1}H NMR studies reveal a 50:43:7 *gg*/*gt*/*tg* ratio for the α anomer and a 56:43:2 ratio for the β anomer.[25] The rotamer population of mannopyranose is similar to that of glucopyranose. However, as will be described later, the results reported here suggest stability of the *tg* form in vacuo. Discrepancies like this are not unique to the work presented here; differences between DFT/molecular mechanics and experimental results have been previously observed.[2]

Recent gas-phase studies using UV and IR ion-dip spectroscopy have experimentally supported previous in vacuo DFT and ab initio calculations.[31–33] From a previous study of cellobiose[6,7] at the B3LYP/6-311++G** level of theory, it has been found that the 'flipped' form is preferred in vacuo over the experimentally observed (solvated) 'normal' form. This 'flipped' form has recently been reported to be observed for another disaccharide in the gas phase (a lactoside derivative).[31]

1.2. Computational methodology

Calculations were carried out using the B3LYP nonlocal exchange functionals and the 6-31+G* and 6-311++G** basis sets as previously described.[1,4–7] Calculations were carried out on Parallel Quantum Solutions software and hardware.[34] Preliminary geometry optimizations were carried out at the B3LYP/6-31+G* level, followed by further optimization at the higher level. All results reported here are at the B3LYP/6-311++G** level of theory. Convergence criteria were set at 1×10^{-6} Hartree and a gradient of less than 3×10^{-4} a.u. Vibrational frequencies were calculated on geometry-optimized structures using an analytical hessian program with the threshold set at 1×10^{-3}, which provided consistent zero vibrational energies, enthalpies and entropies. Results have been displayed using HYPERCHEM v7.5.[35]

Several $^4C_1$ chair conformations of mannopyranose have been considered in this study. The hydroxy group orientation in these studies were taken from lower energy vacuum calculations using the AMB02C force field, an in-house AMBER-based empirical energy force field developed using results from our previous DFT calculations on carbohydrates.[20,21] In several cases, soft minimization was used to maintain desired geometries and minimize the empirical bias prior to the DFT calculations. Geometric assignments were made using improper dihedral angles as described previously.[4,22,23]

2. Results

2.1. Conformations

The $^4C_1$ chair conformations have energies within ~2 kcal/mol of each other and a relative free energy of up to ~2 kcal/mol. In contrast, the $^1C_4$ chair conformations are generally higher in energy (~1.4–7.9 kcal/mol) and higher in relative free energy (4.1–8.3 kcal/mol). The stable boat and skew forms evaluated are ~3.6–8.9 kcal/mol higher in energy. The skew forms are the results of transitions without barrier from modeled, unstable boat forms. The $^4C_1$ chair conformations are the preferred conformations, and a relatively extensive conformational analysis was performed on these structures.

2.2. $^4C_1$ Chair

The effects of anomers, rotamer conformations, and the orientation of the hydroxyls (with an emphasis on the C-2 hydroxyl orientation) were the focus in our $^4C_1$ chair investigation (see Tables 1 and 2, and Figs. 1 and 2). As found in the case of glucopyranose, the $^4C_1$ chair conformation is the lowest energy ring conformation for mannopyranose at this level of theory. Epimerization

Table 1. B3LYP/6-311++G** energies and geometries for α-$^4C_1$ chair conformations of D-mannopyranose[a]

	α-*gg*-$^4C_1$	α-*gg*-$^4C_1$ (HO-2···O-5)	α-*gg*-(O-4)-$^4C_1$	α-*gt*-$^4C_1$	α-*gt*-$^4C_1$ (HO-2···O-5)	α-*tg*-$^4C_1$	α-*tg*-$^4C_1$ (HO-2···O-5)	α-*tg*-$^4C_1$(c)
Energy	−431,351.018	−431,351.841	−431,350.448	−431,351.053	−431,351.808	−431,351.032	−431,351.746	−431,352.076
Δ*E*	1.097	0.274	1.667	1.062	0.307	1.083	0.369	0.039
ZPVE	123.656	123.896	123.979	123.653	123.904	123.858	124.172	123.729
E-ZPVE	−431,227.362	−431,227.945	−431,226.469	−431,227.400	−431,227.904	−431,227. 174	−431,227.574	−431,228.347
Δ*E* (Corr)	1.271	0.688	2.164	1.233	0.729	1.459	1.059	0.286
Enthalpy	132.027	132.155	132.237	132.041	132.152	132.121	132.289	132.054
H-ZPVE	8.371	8.259	8.258	8.388	8.248	8.263	8.177	8.325
Entropy (cal/mol/K)	107.356	106.484	106.934	107.513	106.418	106.497	105.320	107.729
H−*TS* (298 K)	100.035	100.423	100.371	100.002	100.439	100.385	100.904	99.951
ΔG^o_{298}	1.142	0.947	2.048	1.492	0.756	1.478	1.283	0
HO-4···HO-3	2.441	2.464	2.422	2.403	2.433	2.402	2.430	2.377
HO-3···HO-2	2.251	2.315	2.292	2.230	2.301	2.209	2.282	2.242
HO-1···O-5	2.517	2.577	2.581	2.511	2.577	2.507	2.572	2.533
HO-2···O-5		2.530	2.510		2.505		2.523	
HO-6···O-5	2.356	2.431		2.399	2.410			
HO-6···O-4			2.873			2.070	2.079	1.984
O-1–C-1	1.414	1.407	1.409	1.413	1.405	1.414	1.406	1.414
C-5–O-5	1.446	1.448	1.445	1.446	1.450	1.440	1.444	1.434
C-1–O-5	1.407	1.420	1.417	1.408	1.421	1.407	1.421	1.415
C-5–O-5–C-1	116.4	115.4	114.6	115.8	114.8	115.5	114.5	116.1
O-1–C-1–O-5	112.4	112.5	112.8	112.6	112.8	112.5	112.7	111.8
C-1–C-2–C-3	110.5	110.3	110.5	110.7	110.5	110.8	110.6	110.5
α_1	−29.0	−32.7	−32.0	−27.5	−32.8	−26.6	−32.0	−27.6
α_2	−32.4	−30.7	−30.7	−32.0	−29.9	−31.9	−29.9	−32.6
α_3	−32.3	−31.9	−34.6	−34.9	−34.2	−36.1	−35.3	−32.9

[a] All energies are in kcal/mol unless noted otherwise. All bond lengths are in Å.

Table 2. B3LYP/6-311++G** energies and geometries for β-$^4C_1$ chair conformations of D-mannopyranose[a]

	β-*gg*-$^4C_1$	β-*gg* (O-4)-$^4C_1$	β-*gt*-$^4C_1$	β-*tg*-$^4C_1$	β-*tg*-$^4C_1$ (c)
Energy	−431,351.827	−431,350.069	−431,352.002	−431,352.115	−431,352.067
Δ*E*	0.288	2.046	0.113	0	0.048
ZPVE	123.527	123.585	123.541	123.798	123.434
E-ZPVE	−431,228.300	−431,226.484	−431,228.461	−431,28.317	−431,228.633
Δ*E* (Corr)	0.333	2.149	0.172	0.316	0
Enthalpy	131.878	131.934	131.907	132.016	131.386
H-ZPVE	8.351	8.349	8.366	8.218	7.952
Entropy (cal/mol/K)	107.160	107.790	107.265	105.997	104.414
H−*TS* (298 K)	99.944	99.813	99.942	100.429	100.271
ΔG^o_{298}	0.242	0.065	1.869	0.439	0.329
HO-4···HO-3	2.473	2.411	2.432	2.426	2.387
HO-3···HO-2	2.250	2.208	2.231	2.213	2.281
HO-2···HO-1	2.267	2.209	2.247	2.228	2.202
HO-1···O-5	2.369	2.309	2.379	2.341	2.564
HO-2···O-5	3.096	3.059	3.078	3.076	
HO-6···O-5	2.385		2.432		
HO-6···O-4		2.709		2.068	1.974
O-1–C-1	1.400	1.402	1.400	1.400	1.384
C-5–O-5	1.439	1.434	1.440	1.434	1.423
C-1–O-5	1.416	1.414	1.416	1.416	1.431
C-5–O-5–C-1	114.4	113.1	113.6	113.3	114.9
O-1–C-1–O-5	107.8	107.6	108.0	107.8	108.0
C-1–C-2–C-3	109.7	110.2	110.0	110.1	110.8
α_1	−32.1	−28.8	−32.8	−30.8	−30.3
α_2	−30.0	−28.8	−29.4	−29.4	−30.1
α_3	−33.5	−39.6	−36.3	−37.6	−35.3

[a] All energies are in kcal/mol unless noted otherwise. All bond lengths are in Å.

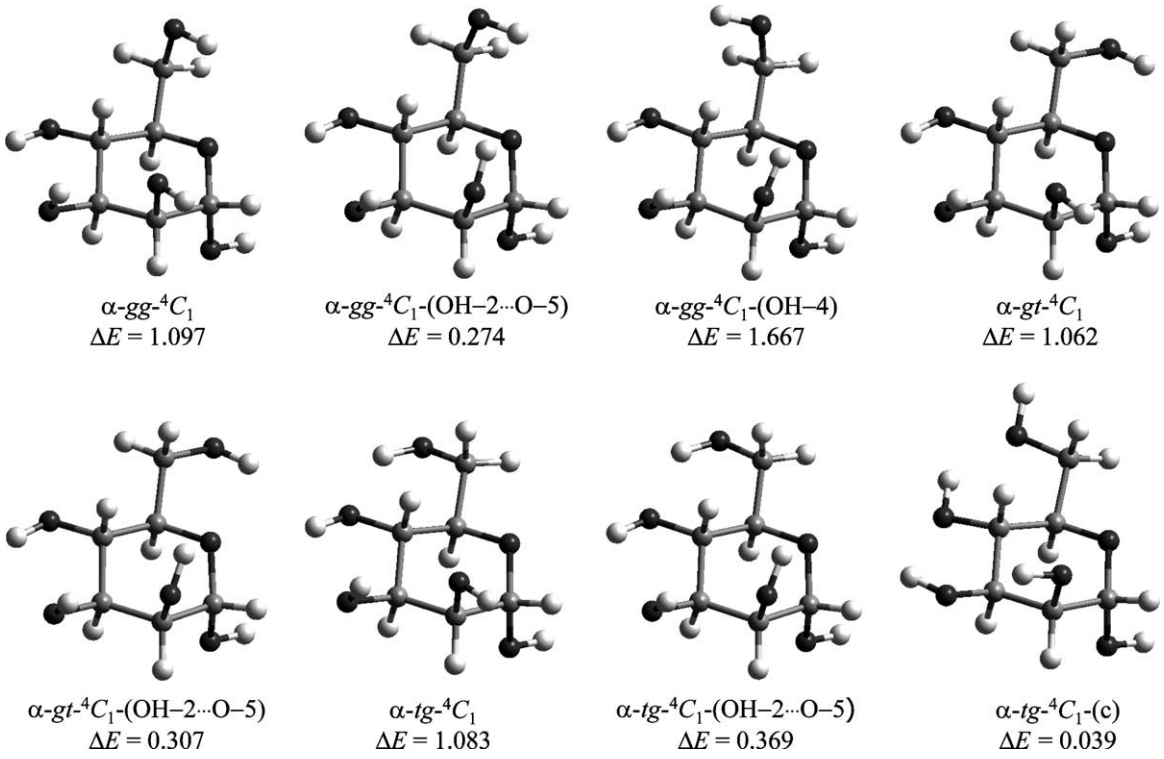

Figure 1. Geometry-optimized α-D-mannopyranose structures in the $^4C_1$ chair conformation. All energies are in kcal/mol.

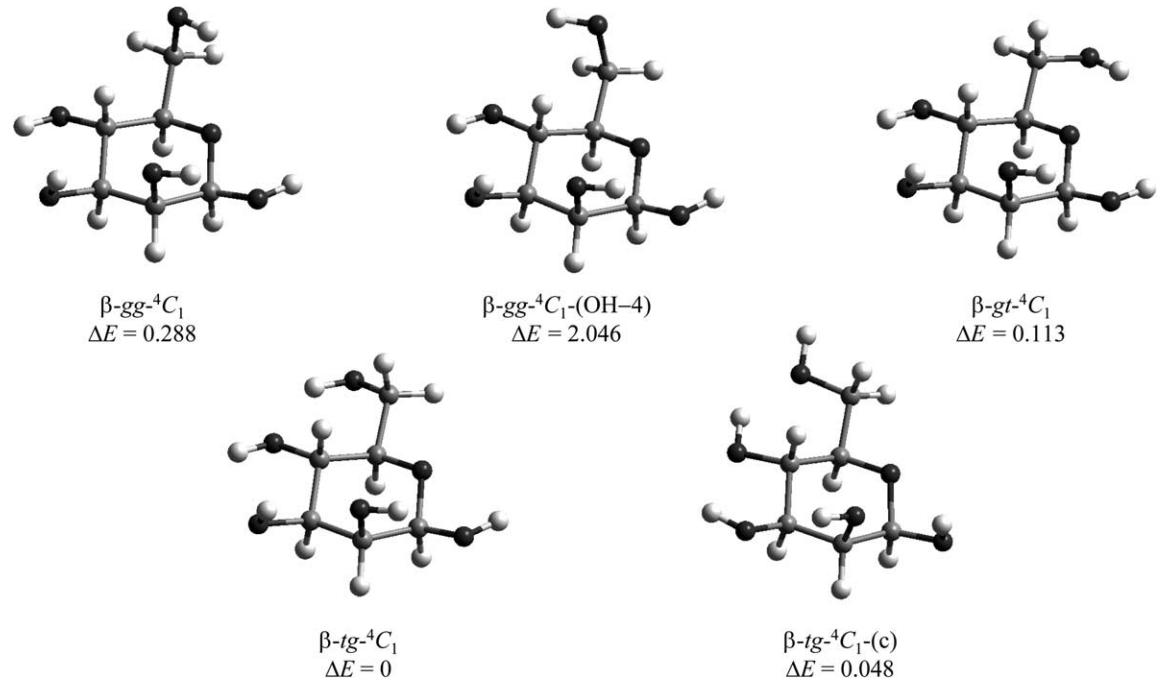

Figure 2. Geometry-optimized β-D-mannopyranose structures in the $^4C_1$ chair conformation. All energies are in kcal/mol.

at the C-2 position results in an increase in overall energy of ~1.3–3.4 kcal/mol in $^4C_1$ chair conformations of mannopyranose over that of the lowest energy glucose structure, the α-*gt*-$^4C_1$. However, contrary to the glucopyranose results, the *tg* rotamers of mannopyranose are slightly lower in energy than their *gg* and *gt* counterparts. The lowest energy structure of mannopyranose at the B3LYP/6-311++G** level of theory is the β-*tg*-$^4C_1$ and is similar to that reported at the B3LYP/6-31G(d) level.[13]

2.3. $^4C_1$ Chair: orientation of hydroxy groups

The orientation of the hydroxy groups and their synergistic, noncovalent interactions are the significant factors in relating geometry to energy for the $^4C_1$ chair conformations. All $^4C_1$ chair conformations in this study contain OH-4···OH-3···OH-2 intramolecular interactions. In addition, the lower energy conformations possess more elaborate networks. For example, the lower energy *tg* rotamers exhibit a ~2 Å hydrogen bond between the OH-6 hydroxymethyl group and the OH-4 hydroxy group resulting in an OH-6···OH-4···OH-3···OH-2 network. The β anomers hold an OH-2···OH-1 interaction forming an OH-4···OH-3···OH-2 interaction for most conformations. The lowest energy conformation of mannopyranose in this investigation, the β-*tg*-$^4C_1$ chair, possesses an extensive OH-6···OH-4···OH-3···OH-2···OH-1 network.

The configuration at the C-2 position in $^4C_1$ chair conformations of mannopyranose places the OH-2 hydroxy group in the axial position, which presents a special emphasis on the orientation of the C-2 hydroxyl in this study. α Anomers of the $^4C_1$ chair type of mannopyranose lack the interaction between the OH-2 hydroxy group and the OH-1 hydroxy group with the C-2 hydroxy group axial 'up' and the C-1 hydroxy group axial 'down' (see Fig. 1). Selected α anomers were geometry optimized with their C-2 hydroxy group interacting with the O-5 ring ether (indicated in Table 1 by (OH-2···O-5)). The formation of the OH-2···O-5 interaction (~2.5 Å) in α anomers lowered overall electronic energy values by ~0.8 kcal/mol, lowered the ZPVE corrected energy by ~0.5 kcal/mol, and the entropy by ~1 cal/mol/K with a more general decrease in free energy. The α anomers with the OH-2···O-5 interaction exhibit a slight increase in enthalpy. However, all β anomer conformers started with the OH-2···O-5 interaction, upon geometry optimization had the OH-2 hydroxy group undergo transition without barrier to an ~2.2 Å OH-2···OH-1 interaction (see Fig. 2). Thus, no stable β anomers were obtained with the OH-2···O-5 interaction.

2.4. $^4C_1$ Chair: rotamer effects

The axial configuration of the hydroxy group at the C-2 position allows for interesting interactions in mannopyranose. The effect of rotamer conformation on energy depends on how the OH-6 hydroxymethyl group interacts with the $^4C_1$ chair mannopyranose ring ether or other ring hydroxy groups. Both α- and β-*gg* and *gt* rotamers in this study exhibit a ~2.4 Å hydrogen bond between the OH-6 hydroxymethyl group and the O-5 ring ether. In contrast, the α- and β-*gg* rotamers, which exhibit an OH-6···OH-4 (~2.8 Å) interaction, are higher in electronic energy and ZPVE corrected energy. The *tg* rotamers were found to be the lowest electronic energy rotamers and are also low in ZPVE corrected energy and free energy. For the α- and β-*tg* rotamers, the conformations with the OH-6···OH-4···OH-3···OH-2 network in the counterclockwise orientation had a ~2.07 Å OH-6···OH-4 bond, while the clockwise orientation possessed a shorter ~1.97 Å interaction.

2.5. $^4C_1$ Chair: anomeric influence

Most $^4C_1$ chair conformations of mannopyranose studied are within ~1 kcal/mol of each other in overall energy with the lowest energy α and β anomers differing by only ~0.04 kcal/mol. The α and β anomers evenly spread across this ~2 kcal/mol range implying that mannopyranose energies are less sensitive to anomeric changes than glucopyranose in the $^4C_1$ chair conformation.[4,5] The anomeric ratio was calculated from the free energy to be 50:50 (α/β). There is an anomeric influence on the C-5–O-5–C-1 bond angle. Most β anomers have a C-5–O-5–C-1 bond angle of ~114 °, while most α anomers without the OH-2···O-5 interaction have a C-5–O-5–C-1 bond angle of ~116°, suggesting that the *trans* effect is the dominant determinate for this internal coordinate. Both anomers of the *tg* rotamers with their pyranose ring hydroxyls in the clockwise orientation posses a C-5–O-5–C-1 bond angle of $\alpha = 116.1°$ and $\beta = \sim 114.9°$. β anomers have a smaller O-1–C-1–O-5 bond angle (~108°) compared to the α anomers (~112.5°), in line with the results found for glucopyranose.[4]

2.6. $^1C_4$ Chair

Transition from the $^4C_1$ chair conformation to the $^1C_4$ chair conformation exchanges the positions of the axial and equatorial substituents, and the effects of this inversion can be seen in the hydroxy group interactions (see Fig. 3 and Table 3). Both the $^4C_1$ and $^1C_4$ chair conformations exhibit a 2.1–2.4 Å OH-3···OH-2 hydrogen bond. However, all $^4C_1$ chair conformations possess OH-4···OH-3 interactions (~2.4 Å), while both the α- and β-forms of the $^1C_4$ chair conformations possess 2.0–2.6 Å OH-2···OH-1 interactions (see Fig. 3). In contrast, for the $^4C_1$ chair conformations, only the β-$^4C_1$ chair conformations contain a 2.2–2.3 Å OH-2···OH-1 interaction. This ring inversion places the hydroxymethyl substituent in the unfavored axial position, and the resulting energies are ~1.4–7.9 kcal/mol above the lowest overall energy $^4C_1$ chair conformation of mannopyranose. The free energies of the $^1C_4$ chair conformations are ~4.1–8.4 kcal/mol higher than the lowest free energy $^4C_1$ chair conformation of mannopyranose.

Similarities between all the $^1C_4$ chair conformations are the interactions between the hydroxy groups at OH-4···O-5, HO-3···OH-2, and HO-2···OH-1. However, unlike the $^4C_1$ chair structures, length of the hydrogen bonds in the β-$^1C_4$ chair varies considerably

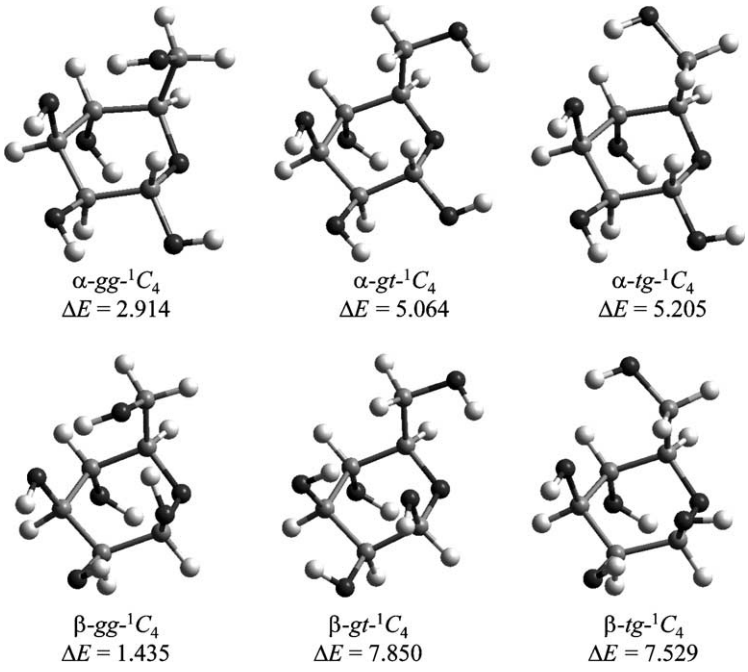

Figure 3. Geometry-optimized structures of α- and β-D-mannopyranose in the $^1C_4$ chair conformations listed in Table 3. All energies are in kcal/mol.

Table 3. B3LYP/6-311++G** energies and geometries for α- and β-$^1C_4$ chair conformations of D-mannopyranose[a]

	α-*gg*-$^1C_4$	α-*gt*-$^1C_4$	α-*tg*-$^1C_4$	β-*gg*-$^1C_4$	β-*gt*-$^1C_4$	β-*tg*-$^1C_4$
Energy	−431,349.201	−431,347.051	−431,346.910	−431,350.679	−431,344.265	−431,344.586
Δ*E*	2.914	5.064	5.205	1.435	7.850	7.529
ZPVE	124.384	123.724	124.275	125.147	123.910	124.269
E-ZPVE	−431,224.817	−431,223.327	−431,222.635	−431,225.533	−431,220.355	−431,220.317
Δ*E* (Corr)	3.816	5.306	5.998	3.100	8.278	8.316
Enthalpy	132.373	132.087	132.416	132.681	132.221	132.467
H-ZPVE	7.989	8.363	8.141	7.534	8.311	8.198
Entropy (cal/mol/K)	103.631	106.889	105.010	100.497	106.793	106.149
H−*TS* (298K)	101.496	100.234	101.123	102.733	100.397	100.835
ΔG^{o}_{298}	4.420	5.308	6.338	4.178	8.257	8.374
HO-3···HO-2	2.190	2.264	2.255	2.186	2.221	2.363
HO-2···HO-1	2.497	2.491	2.545	2.045	2.561	2.020
HO-1···O-5	2.526	2.522	2.482	2.509		2.619
HO-3···HO-1					2.119	
HO-6···HO-3	1.866		2.109	1.806		2.307
HO-4···O-5	2.518	2.551	2.429	2.471	2.676	2.398
HO-6···O-5		2.416			2.456	
HO-1···HO-6				1.750		
O-1–C-1	1.401	1.400	1.400	1.405	1.437	1.423
C-5–O-5	1.423	1.426	1.449	1.443	1.454	1.455
C-1–O-5	1.431	1.429	1.427	1.420	1.398	1.411
C-5–O-5–C-1	115.1	115.0	115.1	119.1	118.5	118.6
O-1–C-1–O-5	108.0	108.1	108.0	114.4	108.9	113.3
C-1–C-2–C-3	111.7	110.8	111.5	115.5	110.7	114.7
α_1	35.3	35.1	31.0	22.5	31.7	18.4
α_2	25.2	28.1	28.8	23.4	30.6	28.2
α_3	31.0	30.1	34.0	34.5	24.2	36.8

[a] All energies are in kcal/mol unless noted otherwise. All bond lengths are in Å.

depending on the rotamer conformations. In this study all α anomers in the $^1C_4$ chair conformation possess a OH-3···OH-2···OH-1 network. The β anomers exhibit more complex hydroxy group interactions than the α anomers. The $^1C_4$ chair conformations exhibit an anomeric influence on bond angle with the C-5–O-5–C-1 bond angle of ∼115° for the α anomers and 118.5–119.1° for the β anomers.

An unexpected, low-energy $^{1}C_4$ chair conformation was discovered when the β-*gg*-$^{1}C_4$ conformation was found to be only ~1.4 kcal/mol higher in total energy than the lowest energy conformation for mannopyranose. The β-*gg*-$^{1}C_4$ conformation has a tight (1.75–2.19 Å) OH-6···OH-3···OH-2···OH-1···OH-6 circular hydrogen bond network. This circular hydrogen bond network contains two favorable antiparallel dipole–dipole interactions between OH-1 and OH-3, and the OH-2 and OH-6 hydroxyls. Antiparallel dipole–dipole interactions of this type have been shown to be overestimated in popular semiempirical methods,[36] but appear to be well treated at the DFT level used here. The effects of the tight interaction can be seen in the entropic terms, where the β-*gg*-$^{1}C_4$ conformation has the lowest entropy (100.497 cal/mol) of all the chair conformations of mannopyranose in this study. In addition the β-*gg*-$^{1}C_4$ conformation is the lowest in free energy of all the $^{1}C_4$ chair conformations found in this investigation.

2.7. Boat and skew forms

Rotamers of the $^{3,O}B$, $B_{3,O}$ and interesting rotamers of the $^{1,4}B$ and $B_{1,4}$ were geometry optimized, and the energies and geometries of the structures are shown in Table 4 (see Figs. 4–6). Many boat forms were not stable and went through transitions without barrier to skew forms or other boat forms.

2.8. Boat and skew forms: $^{3,O}B$ boat

The α-*gt*-$^{3,O}B$ is a stable 'hardboat'-like form, while the *gg* and *tg* rotamers of the initial α-$^{3,O}B$ structure went through a transition without barrier to another boat form, the $B_{1,4}$ boat. The α-*gt*-$^{3,O}B$ boat maintains its $^{3,O}B$ boat form and lacks the OH-4···OH-1 hydrogen bond (~2.0–2.2 Å) found in the *gg* and *tg* forms of the optimized α-$B_{1,4}$ boats. The α-*gt*-$^{3,O}B$ boat conformation contains an OH-6···O-5 interaction (~2.5 Å) between the hydroxymethyl substituent and the ring ether.

Table 4. B3LYP/6-311++G** energies and geometries for skew and boat conformations of D-mannopyranose[a]

Geometry optimized conformations	Starting conformations	α_1	α_2	α_3	ΔE
α-*gg*-$B_{1,4}$	α-*gg*-$^{3,O}B$	−52.7	47.7	0.1	3.645
α-*gt*-$^{3,O}B$		−18.2	60.8	−48.8	7.074
α-*tg*-$B_{1,4}$	α-*tg*-$^{3,O}B$	−48.4	61.4	−12.8	8.860
β-*gg*-$^{1}S_5$	β-*gg*-$^{3,O}B$	53.6	10.2	−54.8	5.031
β-*gt*-$^{1}S_5$	β-*gt*-$^{3,O}B$	53.7	9.5	−56.4	5.379
β-*tg*-$^{1}S_5$	β-*tg*-$^{3,O}B$	−54.5	8.5	−57.4	5.181
α-*gg*-$^{1}S_3$	α-*gg*-$B_{3,0}$	52.4	−60.1	4.0	8.545
α-*gg* (O2)-$B_{3,O}$		14.7	−63.1	35.2	8.815
α-*gt*-$^{1}S_3$	α-*gt*-$B_{3,O}$	48.2	−63.2	7.9	8.067
α-*tg*-$^{1}S_3$	α-*tg*-$B_{3,O}$	60.7	−55.6	−3.5	7.041
β-*gg*-$B_{3,O}$		27.5	−31.7	27.5	5.453
β-*gt*-$B_{3,O}$		14.4	−61.7	39.5	6.143
β-*tg*-$^{1}S_3$	β-*tg*-$B_{3,O}$	54.6	−60.3	−14.1	4.764
α-*gt*-$^{1}S_3$	α-*gt*-$^{1,4}B$	59.0	−56.7	−1.3	6.366
α-*tg*-$B_{2,5}$	α-*tg*-$^{1,4}B$	22.2	31.1	−65.7	4.662
α-*gg* (O-3)-$^{5}S_1$	α-*gg* (O-3)-$B_{1,4}$	−57.0	11.7	33.4	3.847

[a] All energies are in kcal/mol.

2.9. Boat and skew forms: $B_{1,4}$ boat

The *gg* and *tg* rotamers of the α-$^{3,O}B$ investigated went through transitions without barrier to the $B_{1,4}$ boat form despite differences in their hydrogen bond network and rotamer conformation (See Table 4). The lowest energy conformation of the $B_{1,4}$ boat structures is the α-*gg*-$B_{1,4}$ boat, and this structure contains a cooperative OH-2···OH-3···OH-6O-5 network as well as a OH-4···OH-1 hydrogen bond. This is in contrast to the α-*gt*-$^{3,O}B$ and α-*tg*-$B_{1,4}$ boat rotamers that have their

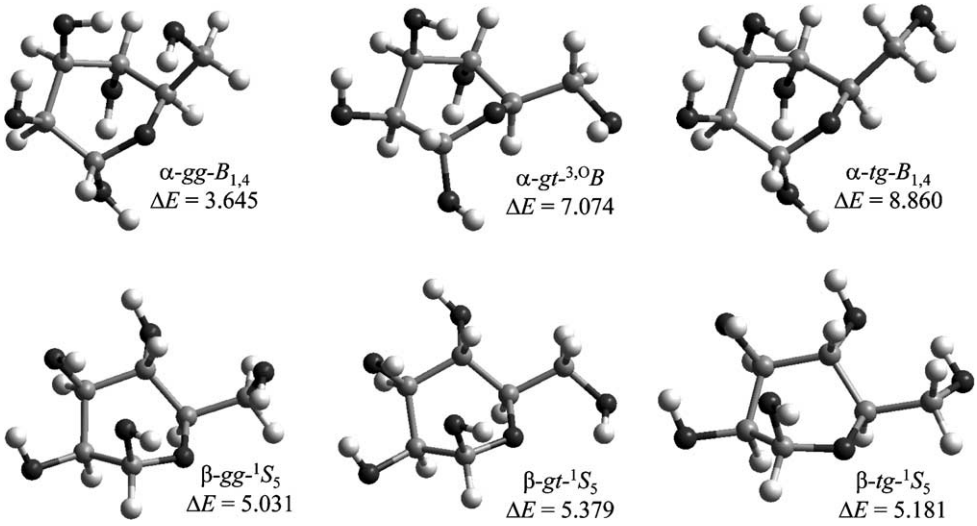

Figure 4. Geometry-optimized structures of α- and β-D-mannopyranose listed in Table 4 that were initially in the $^{3,O}B$ boat form prior to geometry optimization. All energies are in kcal/mol.

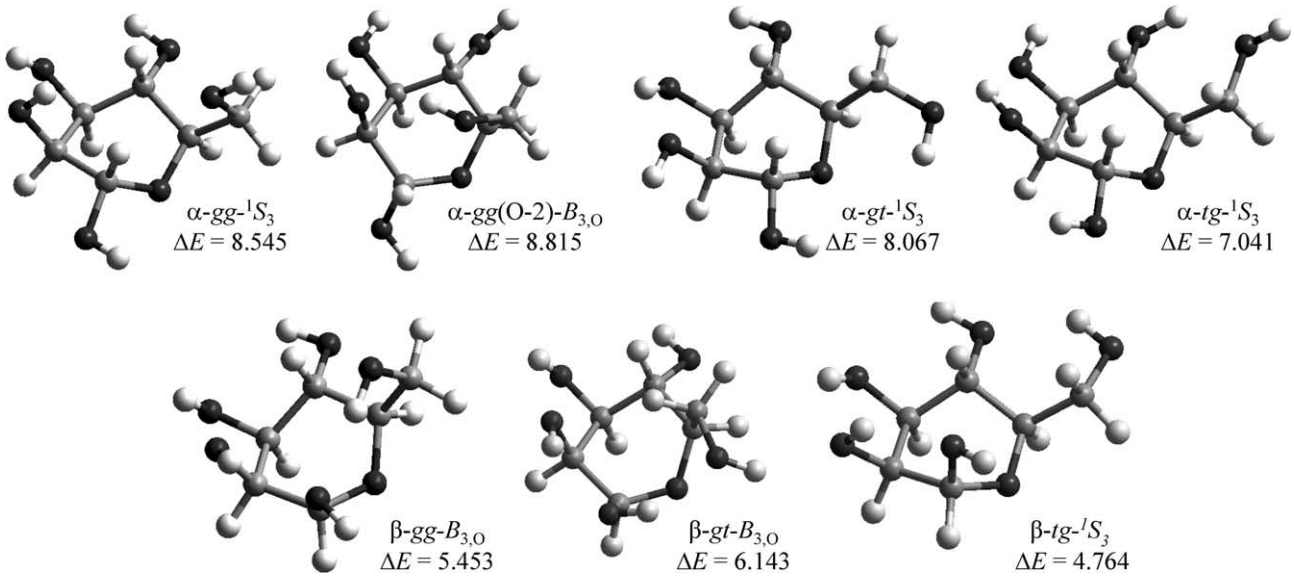

Figure 5. Geometry-optimized structures of α- and β-D-mannopyranose listed in Table 4 that were initially in the $B_{3,O}$ boat form prior to geometry optimization. All energies are in kcal/mol.

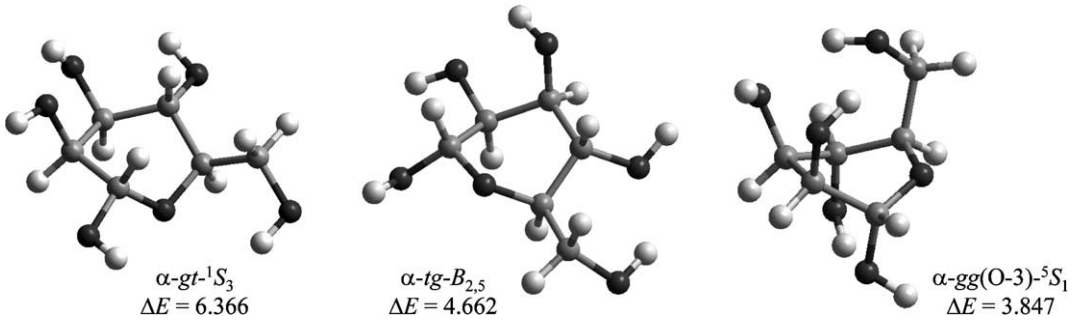

Figure 6. Additional geometry-optimized structures from Table 4. All energies are in kcal/mol.

3-hydroxy group interacting with the O-5 ring ether to form an OH-3···O-5 hydrogen bond across the pyranose ring.

2.10. Boat and skew forms: $B_{2,5}$ boat

The $B_{2,5}$ boat is the result of a transition without barrier from a selected α-*tg*-$^{1,4}B$ boat conformation. The resulting α-*tg*-$B_{2,5}$ boat conformation possesses an OH-6···OH-4···OH-3···OH-2···O-5 hydrogen bond network in the counterclockwise orientation. The α-*tg*-$B_{2,5}$ boat is one of the lower energy boat forms (ΔE = ~4.7 kcal/mol).

2.11. Boat and skew forms: $B_{3,O}$ boat

The α-*gg* (O-2)-$B_{3,O}$ boat conformation is the only α-$B_{3,O}$ boat form in the investigation that maintained the $B_{3,O}$ boat form upon geometry optimization. Despite favorable interactions, including an OH-6···OH-2 hydrogen bond and an OH-6···OH-2···OH-3···OH-4 counterclockwise network, this boat form is relatively high in energy.

The *gg* and *gt* rotamers of the β-$B_{3,O}$ 'softboats' in this investigation maintained their $B_{3,O}$ boat geometries. These β-$B_{3,O}$ softboats were between 5.4 and 6.2 kcal/mol higher in energy than the lowest energy conformations of mannopyranose in this study. One commonality between the *gg* and *gt* β-$B_{3,O}$ boats is the OH-4···OH-3···OH-2···OH-1 network.

2.12. Boat and skew forms: $^1S_3$ skew form

Five $^1S_3$ skew forms were identified and three of the $^1S_3$ skew forms were the result of a transition without barrier from the α-$B_{3,O}$ boat form. These $^1S_3$ skew forms

have energies ~6–9 kcal/mol higher than that of the lowest energy mannopyranose structure.

All of the α-$B_{3,O}$ boat forms have dissimilar intramolecular interactions. The α-*gg*-$^{1}S_3$ and α-*gt*-$^{1}S_3$ originating from the α-$B_{3,O}$ boat form contain an OH-4···OH-3···OH-2 network in the counterclockwise orientation. In contrast, the α-*tg*-$^{1}S_3$ possesses an OH-1···OH-2 OH-3···OH-4···OH-6 clockwise network. However the α-$B_{3,O}$ boat forms, which went through the transition without barrier to the $^{1}S_3$ skew forms, lack the OH-6···OH-2 hydrogen bond present in the stable α-*gg*-$B_{3,O}$ boat conformation, indicating the importance of the OH-6···OH-2 hydrogen bond in maintaining the $B_{3,O}$ boat conformation.

One $^{1}S_3$ skew form discovered was the result of a geometry optimization of a α-*gt*-$^{1,4}B$ boat conformation. This resulting α-*gt*-$^{1}S_3$ skew form is lower in energy by ~0.6–2.2 kcal/mol than the other α-$^{1}S_3$ skew forms. This $^{1}S_3$ skew form possesses a complicated set of intramolecular interactions.

Another $^{1}S_3$ skew form is the result of a transition without barrier from the β-*tg*-$B_{3,O}$ boat form. While the hydroxymethyl group substituent of the *gg* and *gt* rotamers of the β-$B_{3,O}$ boats form an OH-6···O5 interaction, the hydroxymethyl group of the *tg* rotamer interacts with the extended network forming an OH-6···OH-4···OH-3···OH-2···OH-1 network. This network resulted in a change in ring geometry to the β-*tg*-$^{1}S_3$ conformer, and this conformation is lower overall in energy than the stable β-$B_{3,O}$ boat forms. The *tg* rotamer has an overall energy difference of ~4.8 kcal/mol above the lowest energy structure for mannopyranose, while the stable β-$B_{3,O}$ *gg* and *gt* rotamers are an additional ~0.7–1.4 kcal/mol higher in energy.

2.13. Boat and skew forms: $^{5}S_1$ skew form

The α-*gg* (O-3)-$^{5}S_1$ conformation is the result of a geometry optimization of an α-*gg* (O-3)-$^{1,4}B$ boat. This is the lowest energy (ΔE = ~3.8 kcal/mol) skew form. Interesting aspects of this conformation are the position of the hydroxymethyl substituent and a complicated hydrogen-bonding pattern, including an OH-6···OH-3···OH-2···OH-6 circular network and an OH-4···OH-1 hydrogen bond.

2.14. Boat and skew forms: $^{1}S_5$ skew form

The three $^{1}S_5$ skew forms identified in this investigation are the result of geometry optimization of the three rotamers of the β-$^{3,O}B$ 'hardboat' form investigated. The three skew forms are similar in relative energy (ΔE = ~5.0–5.4 kcal/mol). The three rotamers possess similar OH-2···OH-3···OH-1 networks. The *gt* and *tg* rotamers form interactions between the hydroxymethyl group and the ring ether, while the *tg* rotamer has an OH-6···OH-4 hydrogen bond (2.07 Å).

3. Conclusions

This study has brought to light several results that deserve further discussion. One important observation is that small changes in hydroxy group interactions can lead to drastic changes in geometries and energies upon geometry optimization. In the study of the α-$B_{3,O}$ boat forms, a boat conformation with an OH-6···OH-2 hydrogen bond interaction maintained the boat form, while other conformations lacking this interaction passed through a transition without barrier to skew forms.

Further, in our $^{4}C_1$ chair study several of the *tg*-$^{4}C_1$ chair conformations have similar energies, despite significant differences in their hydroxy group orientation. This is an example of how energies and energy minima are results of the whole structure, and the effects on the whole structure must be taken into consideration during the interpretation of specific stabilizing influences.

Of particular interest in the mannopyranose results presented here is the comparison with our previous studies of glucopyranose by DFT at a high level of theory.[4] Although both glucopyranose and mannopyranose have the $^{4}C_1$ chair structures as the lowest energy ring conformation, the two different molecules show dissimilar preferences for rotamer conformation and anomer preference in vacuo.

Configuration at the C-1 position has less of an effect on energies in mannopyranose with low-energy α and β anomers for the $^{4}C_1$ chair structures investigated. For these mannopyranose calculations in vacuo, the lack of an anomeric preference can be attributed to the importance of the OH-2···OH-1 interaction. The effect of epimerization at the C-2 position can be seen in the boat and skew form results—where mannopyranose had no stable $^{3,O}B$ boats and few stable $B_{3,O}$ boats, in contrast to the glucopyranose results.

In this high-level DFT study, intramolecular interactions, including hydrogen bonding and cooperative hydrogen bonding, are significant factors in determining relative energies and ring geometries in vacuo. Discrepancies between anomeric ratio and rotamer preferences between these calculations and previous experimental results may be explained by hydration effects, where water may act as a explicit hydrogen bond donor or acceptor in a vast number of positions. Water, acting as both a hydrogen bond donor and acceptor, has been observed in X-ray crystal structures of carbohydrates.[28] Explicit water calculations have also been reported to account for similar discrepancies in the anomeric ratio for glucopyranose calculations in vacuo.[5]

References

1. Momany, F. A.; Willett, J. L. *J. Comput. Chem.* **2000**, *21*, 1204–1219.
2. Lii, J.-H.; Ma, B.; Allinger, N. L. *J. Comput. Chem.* **1999**, *120*, 1593–1603.
3. Hoffman, M.; Rychlewski, J. *Comput. Methods Sci. Technol.* **2000**, *6*, 61–64.
4. Appell, M.; Strati, G. L.; Willett, J. L.; Momany, F. A. *Carbohydr. Res.* **2004**, *339*, 537–551.
5. Momany, F. A.; Appell, M. A.; Strati, G. L.; Willett, J. L. *Carbohydr. Res.* **2004**, *339*, 553–567.
6. Strati, G. L.; Willett, J. L.; Momany, F. A. *Carbohydr. Res.* **2002**, *337*, 1833–1849.
7. Strati, G. L.; Willett, J. L.; Momany, F. A. *Carbohydr. Res.* **2002**, *337*, 1851–1859.
8. Wieberg, K. B. *J. Comput. Chem.* **2004**, *25*, 1342–1346.
9. Hemmingsen, L.; Madsen, D. E.; Esbensen, A. L.; Olsen, L.; Engelsen, S. B. *Carbohydr. Res.* **2004**, *339*, 937–948.
10. Bernardi, A.; Colombo, A.; Sanchez-Medina, I. *Carbohydr. Res.* **2004**, *339*, 907–928.
11. Dowd, M. K.; French, A. D.; Reilly, P. J. *Carbohydr. Res.* **1994**, *264*, 1–19.
12. Kuttel, M.; Brady, J. W.; Naidoo, K. J. *J. Comput. Chem.* **2003**, *23*, 1236–1243.
13. Wong, C. H. S.; Siu, F. M.; Ma, N. L.; Tsang, C. W. *J. Mol. Struct. (Theochem)* **2001**, *536*, 227–234.
14. Lii, J.-H.; Chen, K.-H.; Durkin, K. A.; Allinger, N. L. *J. Comput. Chem.* **2003**, *24*, 1473–1489.
15. Lii, J.-H.; Chen, K.-H.; Allinger, N. L. *J. Comput. Chem.* **2003**, *24*, 1504–1513.
16. Ma, B.; Schaefer, H. F.; Allinger, N. L. *J. Am. Chem. Soc.* **1998**, *120*, 3411–3422.
17. Jeffrey, G. A.; Pople, J. A.; Radom, L. *Carbohydr. Res.* **1974**, *38*, 81–95.
18. Hadjduk, P. J.; Horita, D. A.; Lerner, L. E. *J. Am. Chem. Soc.* **1993**, *120*, 9196–9201.
19. Damm, W.; Frontera, A.; Tirado-Rives, J.; Jorgensen, W. L. *J. Comput. Chem.* **1997**, *18*, 1955–1970.
20. Momany, F. A.; Willett, J. L. *Carbohydr. Res.* **2000**, *326*, 194–209.
21. Momany, F. A.; Willett, J. L. *Carbohydr. Res.* **2000**, *326*, 210–226.
22. Joshi, N. V.; Rao, V. S. R. *Biopolymers* **1979**, *18*, 2993–3004.
23. Qasba, P. K.; Balaji, P. V.; Chandrasekaran, R. In *Conformation of Carbohydrates*; Rao, V. S. R., Ed.; Harwood Academic: Amsterdam, 1998; p 56.
24. Tvaroška, I.; Taravel, F. R.; Utille, J. P.; Carver, J. P. *Carbohydr. Res.* **2002**, *337*, 353–367.
25. Bock, K.; Duus, J. Ø. *J. Carbohydr. Chem.* **1994**, *13*, 513–543.
26. Angyal, S. J. *Angew. Chem., Int. Ed. Engl.* **1969**, *8*, 157–166.
27. Jeffrey, G. A. *Acta Crystallogr.* **1990**, *B46*, 89–103.
28. Imberty, A.; Chanzy, H.; Pérez, S.; Buléon, A.; Tran, V. *J. Mol. Biol.* **1988**, *201*, 365–378.
29. Longchambon, F.; Gillier-Pandraud, H. *Acta Crystallogr.* **1977**, *B32*, 1822–1826.
30. van Eijck, B. P.; Mooij, W. T. M.; Kroon, J. *J. Phys. Chem. B* **2001**, *105*, 10573–10578.
31. Jockusch, R. A.; Kroemer, R. T.; Talbot, F. O.; Snoek, L. C.; Carcabal, P.; Simons, J. P.; Havenith, M.; Bakker, J. M.; Compagnon, I.; Meijer, G.; von Helden, G. *J. Am. Chem. Soc.* **2004**, *126*, 5709–5714.
32. Jockusch, R. A.; Kroemer, R. T.; Talbot, F. O.; Simons, J. P. *J. Phys. Chem. A* **2003**, *107*, 10725–10732.
33. Talbot, F. O.; Simons, J. P. *Phys. Chem. Chem. Phys.* **2002**, *4*, 3562–3565.
34. PQS Ab Initio Program Package, Parallel Quantum Solutions, 2013 Green Acres, Suite E, Fayetteville, AR 72703, USA.
35. HyperChem 7.5, Hypercube, Inc., 115 NW 4th Street, Gainesville, FL 32601, USA.
36. Berski, S.; Zszislaw, L. *Comput. Chem.* **1997**, *21*, 347–354.